

Abnormally Long-Range Diamagnetic Anisotropy Induced by Cyclic d_δ - p_π π Conjugation within a Six-Membered Dimolybdenum/Chalcogen Ring

Zhong Fei Tan,[†] Chun Y. Liu,^{*,†,‡} Ziyun Li,[†] Miao Meng,[‡] and Ng Seik Weng[§]

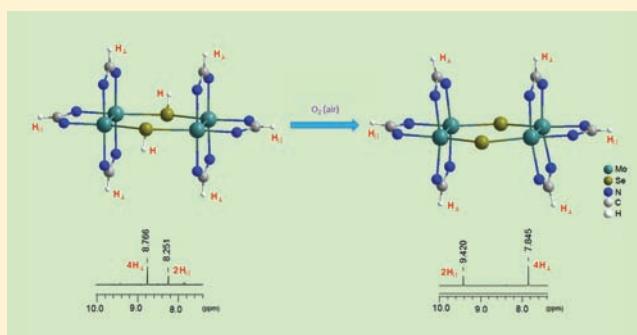
[†]Department of Chemistry, Tongji University, Shanghai 200092, People's Republic of China

[‡]Department of Chemistry, Jinan University, Guangzhou 510632, People's Republic of China

[§]Department of Chemistry, University of Malaya, Kuala Lumpur 50603, Malaysia

Supporting Information

ABSTRACT: Incorporating two quadruply bonded dimolybdenum units $[\text{Mo}_2(\text{DAniF})_3]^+$ (ancillary ligand DAniF = N,N' -di-*p*-anisylformamidinate) with two hydroselenides (SeH^-) gave rise to $[\text{Mo}_2(\text{DAniF})_3]_2(\mu\text{-SeH})_2$ (**1**). With the molecular scaffold remaining unchanged, aerobic oxidation of **1**, followed by autodeprotonation, generated $[\text{Mo}_2(\text{DAniF})_3]_2(\mu\text{-Se})_2$ (**2**). The two complexes share a common cyclic six-membered Mo_2/Se core, but compound **2** is distinct from **1** by having structural, electronic, and magnetic properties that correspond with aromaticity. Importantly, the aromatic behaviors for this non-carbon system are ascribable to the bonding analogy between the δ component in a Mo-Mo quadruple bond and the π component in a C-C double bond. Cyclic π delocalization via d_δ - p_π conjugation within the central unit, which involves six π electrons with one electron from each of the Mo_2 units and two electrons from each of the bridging atoms, has been confirmed in a previous work on the oxygen- and sulfur-bridged analogues (Fang, W.; et al. *Chem.—Eur. J.* **2011**, *17*, 10288). Of the three members in this family, compound **2** exhibits an enhanced aromaticity because of the selenium bridges. The remote in-plane and out-of-plane *methine* (ArNCHNAr) protons resonate at chemical shifts (δ) 9.42 and 7.84 ppm, respectively. This NMR displacement, $\Delta\delta = 1.58$ ppm, is larger than that for the oxygen-bridged (1.30 ppm) and sulfur-bridged (1.49 ppm) derivatives. The abnormally long-range shielding effects and the large diamagnetic anisotropy for this complex system can be rationalized by the induced ring currents circulating the $\text{Mo}_2/\text{chalcogen}$ core. By employment of the McConnell equation $\{\Delta\sigma = \Delta\chi[(1 - 3 \cos 2\theta)/3R^3N]\}$, the magnetic anisotropy ($\Delta\chi = \chi_\perp - \chi_\parallel$) is estimated to be -414 ppm cgs, which is dramatically larger than -62.9 ppm cgs for benzene, the paradigm of aromaticity. In addition, it is found that the magnitude of $\Delta\chi$ is linearly related to the radius of the bridging atoms, with the selenium analogue having the largest value. This aromaticity sequence is in agreement with that for the chalcogen-containing aromatic family, e.g., furan < thiophene < selenophene.



INTRODUCTION

Aromaticity is one of the most important fundamental concepts in modern chemistry,¹ which stemmed from questioning the peculiar structure of benzene (C_6H_6). Kekulé's 1865 proposal of the ringlike structure for this molecule² sparked continuous intensive research aimed at new aromatic compounds and insightful understanding of aromaticity.³ Today, this field has crossed the organic border and become a largely expanded interplaying realm for both experimental and theoretical chemists. By modification of the aromatic hydrocarbon frames with non-carbon elements, a new area, so to speak, heteroaromaticity, has been developed. Replacement of a CH group in benzene with main-group elements gives rise to molecules such as pyridine, phosphabenzene, arsabenzene, and silabenzene.⁴ Analogues of benzene having one transition-metal atom with ancillary ligands, which thereby belong to inorganic or organometallic compounds, were predicted by Thorn and

Hoffmann based on their theoretical examination.⁵ Since "osmabenzene" was first reported by Roper et al. in 1982,⁶ a variety of metallabenzene containing various transition metals, for example, osmabenzene,⁷ iridabenzene,⁸ and platinabenzene,⁹ have been synthesized and investigated.

A question that has to be confronted in the study on these "modified benzenes" would be, "Does the molecule retain its aromaticity?". A more scientific approach to this type of question could be, "How well does the introduced atom conduct the cyclic π delocalization?". For the heterobenzenes with a main-group element involved, their aromaticity is generally retained because the p_π - p_π conjugation is similar to that occurring in the benzene ring, although the degree may vary depending on the non-carbon atom introduced.¹⁰

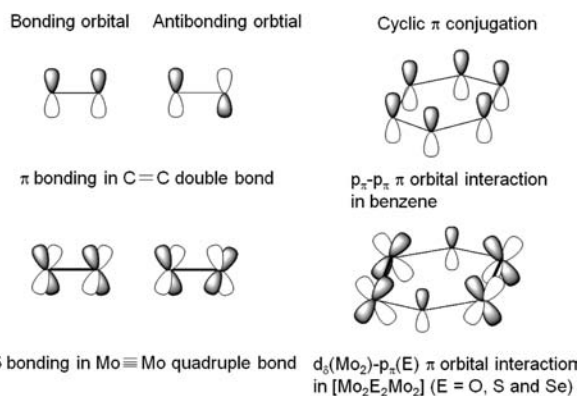
Received: October 11, 2011

Published: February 1, 2012

However, the aromaticity for transition-metal-containing metalabenzene has been an issue that has raised significant controversy. The complicity results obviously from the metal d orbitals involved in π delocalization within the six-membered ring, namely, d–p π conjugation.¹¹ Earlier work considered six π electrons in the ring as occurring in benzene, four from the carbon p_π moiety and two from the filled metal d_{xz} orbital.⁵ Recently, some researchers believed that metallabenzene satisfies Hückel's $(4n + 2)$ ¹² with 10 π electrons ($n = 2$).¹³ The latest work demonstrated that the aromaticity for this class of molecules is determined by the number of outer-shell electrons of the metal center. The 18-electron complexes are aromatic, while the 16-electron molecules are antiaromatic.¹⁴ On the other hand, owing to the local magnetic anisotropy of the transition-metal center, the popular methods for quantifying the aromaticity of a molecule, such as calculations of the nucleus-independent chemical shift (NICS)¹⁵ and magnetic susceptibility anisotropy ($\Delta\chi$), have severe limitations. Nevertheless, metallabenzenes may be aromatic, but the degree of aromaticity varies depending on the electronic configuration of the metal center.¹⁶

It is interesting to note that the δ component of the quadruple bond in a dimetal unit, e.g., $\text{Mo}\equiv\text{Mo}$ in Mo_2 ,¹⁷ resembles the π component of a C=C double bond. They are both two-center, three-electron ($2c-2e$) bonds formed by the highest occupied molecular orbital.¹⁸ More importantly, the two bonds (π and δ), including their bonding and antibonding molecular orbitals (MOs), are symmetry-adaptable for π interaction with the bonded atoms (Scheme 1). This bonding

Scheme 1. Bonding Analogy between the δ Orbital of a Mo–Mo Quadruple Bond and the π Orbital of a C–C Double Bond

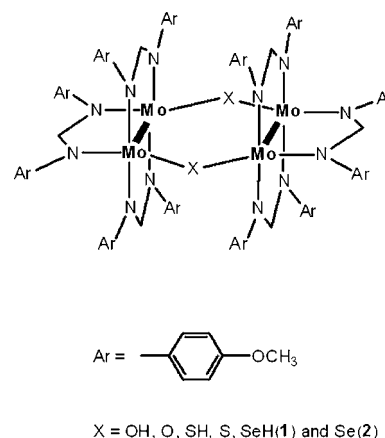


analogy between p_π and d_δ inspired us to examine the aromaticity for molecules or fragments derived from quadruply bonded dimolybdenum (Mo_2) units, so-called “ δ aromaticity”. The additional reason for using Mo_2 units to construct aromatic species is that it has a well-defined closed-shell electronic configuration in which the d electrons fully occupy the whole set of metal–metal bonding orbitals, e.g., $\sigma^2\pi^4\delta^2$. The “simplicity” of a dimetal unit in the electronic structure should be greatly beneficial to the orbital analysis regarding the aromaticity of the derived molecules.

In recent work, we reported two pairs of chalcogen-bridged Mo_2 complexes, $[\text{Mo}_2(\text{DAniF})_3]_2(\mu\text{-EH})_2$ and $[\text{Mo}_2(\text{DAniF})_3]_2(\mu\text{-E})_2$ (DAniF = *N,N'*-di-*p*-anisylformamidinate and E = O and S),¹⁹ in which the six-membered Mo_2/E core exhibits typical aromatic character as gauged by conven-

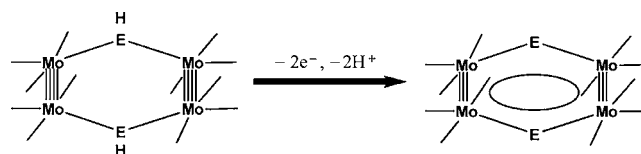
tional aromatic criteria, including ring planarity, bond equalization, full electron delocalization, and abnormal chemical shifts for the protons nearby. As shown in Scheme 2, these

Scheme 2. Molecular Framework for the $\text{Mo}_2/\text{Chalcogen Clusters}$



compounds share a unique molecular scaffold, of which the central moiety is a hexagon consisting of two single-atom-bridged Mo_2 units. The two molecules in each pair differ by the core structure $[\text{Mo}_2(\text{EH})_2\text{Mo}_2]$ for one and $[\text{Mo}_2\text{E}_2\text{Mo}_2]$ for the other. The transformation of the complex core is depicted in Scheme 3. The relationship between these paired molecules

Scheme 3. Transformation of the Complex Core from Non-Aromatic to Aromatic



is quite similar to that between Dewar benzene and benzene,²⁰ a well-known pair of valence-bond isomers that differ from each other in aromaticity. The closed-shell consideration for the core composed of two Mo_2^{5+} units is supported by experimental observations and calculations at the density functional theory (DFT) level, whereas the possibility of a diradical ground state cannot be ruled out. Theoretical work has shown that the $[\text{Mo}_2\text{E}_2\text{Mo}_2]$ core resembles benzene by having six π -type MOs with the same symmetry and electron population.¹⁹ Importantly, in this non-carbon aromatic system, cyclic π delocalization is attributed to $d_\delta(\text{Mo}_2)\text{-}p_\pi(\text{E})$ conjugation, which involves six π electrons with two electrons from the δ (Mo_2) orbitals and four electrons from the p_π (E) orbitals.

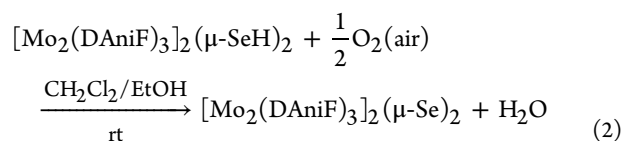
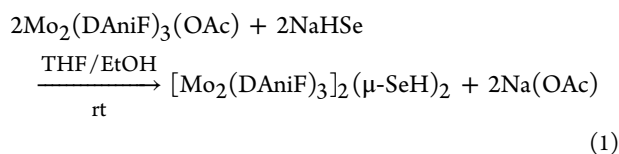
Furthermore, the availability of two molecules in a pair, which behave contrarily in terms of aromaticity, allows us to examine the aromaticity for such a sophisticated non-carbon system by taking a straightforward approach. Accompanying the alternation of the core, the *methine* protons (ArNCHNAr) from the parallel and perpendicular DAniF ligands, denoted as H_\parallel and H_\perp accordingly, exhibit downfield- and upfield-shifted NMR signals, respectively. This observation suggests that the in-plane (H_\parallel) and out-of-plane (H_\perp) protons are located in the negative and positive zones in an anisotropic magnetic field and, therefore, experience deshielding and shielding, respectively. This phenomenon is exactly as predicted by the ring-

current model.²¹ Therefore, the experimental results observed in this non-carbon aromatic system support the ring-current model that has been challenged occasionally by theoretical work.²²

To fulfill a systematic study and gain additional understanding, in the present work, we extended the Mo₂/chalcogen series by adding the selenium-bridged pair [Mo₂(DAniF)₃]₂(μ-SeH)₂ (**1**) and [Mo₂(DAniF)₃]₂(μ-Se)₂ (**2**), which are the first Mo₂ “dimers of dimers” derived by Mo–Se bonds. The two complexes have the same molecular scaffold as the oxygen and sulfur analogues (Scheme 2), with subtle differences in their structural parameters. For compound **2**, the NMR chemical shifts (δ) for the in-plane and out-of-plane *methine* protons are separated by 1.58 ppm, larger than those found for the oxygen- and sulfur-bridged analogues.¹⁹ In this study, in particular, the abnormally large magnetic anisotropy for the Mo₂/chalcogen clusters has drawn our attention. As is known, in the case of benzene, the protons located at 2.45 Å from the ring center display the NMR chemical shift at ca. 2 ppm downfield of those of ethylene protons. In comparison, the induced magnetic field from the complex core exerts a substantial impact on the remote *methine* protons (4–6 Å from the ring center). The implication of this result could be multifold: a large spatial area for the induced magnetic field, intense ring currents circulating the six-membered [Mo₂E₂Mo₂] core, and a high degree of aromaticity of the central fragment. By employment of the McConnell equation,²³ which has been conventionally used to assess the NMR shielding effect on protons in proximity to an anisotropic group,²⁴ the difference between the diatropic and paratropic components of the diamagnetic susceptibility (Δχ = χ_⊥ – χ_∥) was calculated for each of the three aromatic species. Surprisingly, the estimated Δχ values for the complex series are found in the range of –299 to –414 ppm cgs, which is considerably larger than that for benzene (–62.9 ppm cgs).²⁵ The magnitude of the magnetic anisotropy, as measured by Δχ, is linearly related to the radius of the bridging atoms, with the selenium-bridged species giving the largest value.

RESULTS AND DISCUSSION

Synthetic Consideration. The yellow compound **1** was readily prepared from the reactions shown in eq 1. Sodium hydroselenide NaHSe, which is not commercially available, was prepared by the reaction of sodium borohydride with the element selenium before use. Converged synthesis that led to the formation of the selenium-bridged “dimer of dimers” was achieved because the acetate group in the starting material Mo₂(DAniF)₃(OAc) is more labile than the formamidinate ligands.²⁶ Compound **2** was synthesized by air oxidation of **1** in CH₂Cl₂ solutions, followed by autodeprotonation, as shown in eq 2. It should be noted that **1** is air-sensitive even in the solid state, and its yellow solution turns dark immediately when exposed to air. However, compound **2** can be prepared only via the precursor (**1**). A one-pot reaction by mixing Mo₂(DAniF)₃(OAc) with NaHSe solutions in air produced a yet unidentified black, insoluble amorphous powder. Compound **2** is fairly stable in comparison with **1**.



Structure Characterization. The X-ray crystallographic data for compounds **1** and **2** are given in Table 1, and selected

Table 1. X-ray Crystallographic Data for **1** and **2**

	1·2CH ₂ Cl ₂	2·2CH ₂ Cl ₂
formula	C ₉₂ H ₉₆ Cl ₄ Mo ₄ N ₁₂ O ₁₂ Se ₂	C ₉₂ H ₉₄ C ₁₄ Mo ₄ N ₁₂ O ₁₂ Se ₂
fw	2245.29	2243.27
space group	P $\bar{1}$ (No. 2)	P2 ₁ (No. 4)
a (Å)	13.7167(2)	13.2710(7)
b (Å)	14.1504(2)	13.7390(7)
c (Å)	14.4465(2)	25.720(1)
α (deg)	106.856(2)	90
β (deg)	110.300(2)	92.509(1)
γ (deg)	104.309(2)	90
V (Å ³)	2320.3(5)	4685.0(4)
Z	1	2
T (K)	173	293
d _{calcd} (g cm ⁻³)	1.607	1.590
μ (mm ⁻¹)	1.494	1.480
R1 ^a	0.0468	0.0393
wR2 ^b	0.1490	0.1044
^a R1 = $\sum F_o - F_c / \sum F_o $. ^b wR2 = $[\sum [w(F_o^2 - F_c^2)^2] / \sum [w(F_o^2)^2]]^{1/2}$.		

bond distances and angles are presented in Table 2. As shown in Figure 1, the two compounds have similar molecular frameworks, which is unique for this family of Mo₂/chalcogen clusters, including previously reported oxygen- and sulfur-bridged analogues.¹⁹ The central moiety for the two compounds is a six-membered ring consisting of two selenium-bridged Mo₂ units. Surrounding the core, there are six DAniF ligands to saturate the rest of the equatorial coordination sites of the two Mo₂ units; four of them are perpendicular and two parallel to the ring plane. The striking difference between **1** and **2** resides in the core structure. Compound **1** has the six-membered core formed by two hydroselenyl-bridged Mo₂⁴⁺ units, namely, [Mo₂(SeH)₂Mo₂]. Thus, the Mo₂ unit has a quadruple bond with an electronic configuration of σ²π⁴δ². In the crystal structure, the hydrogen atoms on the hydroselenyl groups (SeH) were located from the electronic density maps and refined with isotropic displacement parameters. The presence of the hydroselenyl bridges in **1** is confirmed by the NMR singlet at –2.39 ppm. The H–Se–Mo angles are measured to be 87.0° and 104.7°, and the H–Se⋯Se angle is 104.7°, while the Se–H bond is 1.344 Å in length. From these structural parameters, one may expect poor electronic communication between the two Mo₂ units through the bridging atoms (selenium).

By close examination, more structural parameter alternations are observed, which reflects the important difference in the electronic property between the two cores. The Mo–Mo bonds in **1** are crystallographically equivalent with a distance of 2.1125(5) Å (Table 2). This length is typical for a quadruply bonded Mo₂⁴⁺ supported by three-atom-bridging ligands¹⁷ and very close to those for the oxygen and sulfur analogues.¹⁹ The Mo–Mo bond distances in **2** increased to 2.1353(7) and 2.1385(7) Å, significantly longer than those in **1**. This result

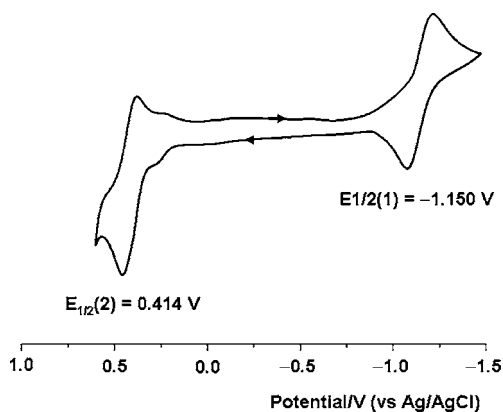


Figure 2. Cyclic voltammogram for **2** showing two reversible processes. Scanning started and ended at -1.474 V, at which potential the neutral analyte is converted to its dianion, proceeding in the direction indicated by the arrows.

Recent studies on a variety of bridged Mo_2 pairs have shown that the potential separation for the two successive redox processes serves as an excellent probe for asserting the extent of electron delocalization.³⁰ The major factors that influence the $\Delta E_{1/2}$ value include (1) the interaction mode between the two Mo_2 units, (2) the electronic property of the linker, and (3) the metal-to-metal nonbonding distance. The potential separation $\Delta E_{1/2}$ of 1.564 V for **2** is exceptionally large compared to those for other Mo_2 “dimers of dimers”.³¹ For instance, in $[\text{Mo}_2(\text{DAniF})_2]_2(\mu\text{-X})_4$ ($\text{X} = \text{OCH}_3, \text{Cl}, \text{Br}, \text{and I}$), direct σ interaction between the d_δ orbitals from the two Mo_2 units is established because of the extremely short metal-to-metal separation, ca. $3.2\text{--}4.0$ Å.³² However, the $\Delta E_{1/2}$ value for such a case was found in the range of $0.440\text{--}0.554$ V, much smaller than 1.564 V observed for **2** and the oxygen- and sulfur-bridged species. Therefore, the very large $\Delta E_{1/2}$ values for this system suggest that electron delocalization through $d_\delta\text{--}p_\pi$ π conjugation is fairly efficient, which facilitates cyclic π delocalization for aromaticity.

Electronic Spectroscopy. Compound **1** shows an electronic spectrum typical for quadruply bonded Mo_2 paddlewheel molecules, as seen in Figure 3. In the spectrum,

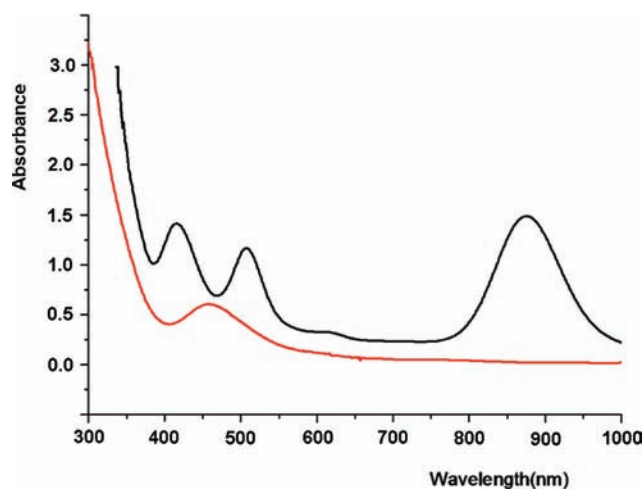


Figure 3. Electronic spectra measured in a CH_2Cl_2 solution for **1** (red) and **2** (black).

the low intense band at 455 nm can be assigned unambiguously to the $\delta \rightarrow \delta^*$ transition, which disappeared in the spectrum of **2**. Compound **2** exhibits three isolated bands in a wide region from 400 to 1000 nm. The spectra of **1** and **2** are similar to those observed for the corresponding oxygen and sulfur analogues. Prior to this work, the characteristic electronic spectra for this system have been discussed in detail based on the computational results.¹⁹ As shown in Figure 3, there is a broad and intense band appearing at 875 nm for compound **2**, which is responsible for its dark color. Theoretical work has confirmed that this band arises from the highest occupied molecular orbital (HOMO) to lowest unoccupied molecular orbital (LUMO) excitation. The HOMO is generated by the out-of-phase combinations of the two δ -bonding orbitals, whereas the LUMO results from the in-phase addition of the two dimetal orbitals but with significant involvement of the p_π (E) orbitals. Therefore, this excitation conventionally refers to metal-to-ligand charge transfer. The oxygen and sulfur analogues show the HOMO–LUMO transition at 725 and 803 nm, respectively. In comparison, an appreciable red shift for this band is observed in the $[\text{Mo}_2(\text{DAniF})_3]_2(\mu\text{-E})_2$ series, with bridging atoms from oxygen to selenium in order.¹⁹ The reduced HOMO–LUMO energy gap for compound **2** confirms that mediation of the selenium bridges gives rise to strong metal-to-metal interaction.

Furthermore, the DFT calculations for this complex system generated six π -type MOs that are similar in symmetry to those for benzene, of which three are occupied and the others unoccupied.¹⁹ However, different from the $p_\pi\text{--}p_\pi$ interaction in benzene, cyclic π conjugation in the Mo_2/E core is attributed to the $d_\delta(\text{Mo}_2)\text{--}p_\pi(\text{E})$ interaction. It is interesting to note that, in the spectrum of **2**, there are three bands arising from excitations between the MOs associated with the π system of the six-membered $[\text{Mo}_2\text{E}_2\text{Mo}_2]$ core. This is also quite similar to the benzene case where three bands, including two E bands at 180 and 200 nm and one B band at 255 nm, are assigned as aromatic–aromatic $\pi \rightarrow \pi^*$ transitions.

NMR Spectroscopy. The ^1H NMR spectra for this complex system are remarkable. First, the oxidized species are diamagnetic, as confirmed by the NMR and magnetic susceptibility measurements for the compound having a $[\text{Mo}_2\text{S}_2\text{Mo}_2]$ core,¹⁹ although they formally have two bridged Mo_2^{5+} units with an electronic configuration of $\sigma^2\pi^4\delta^1$. Second, upon aerobic oxidation/deprotonation, the NMR signals for the two sets of *methine* (ArNCHNAr) protons were displaced by about 1 ppm, although these protons are located far away from the center of the $\text{Mo}_2/\text{chalcogen}$ core. More importantly, those parallel to the core, H_{\parallel} , and those perpendicular to the core, H_{\perp} , exhibit downfield and upfield chemical shifts, respectively, which are separated by more than 1 ppm. There are relatively few organic arenes,³³ which feature two types of protons located in and above the ring plane so that the aromaticity can be judged by NMR based on the ring-current model. From this point of view, this non-carbon aromatic system is quite unique. We have delivered a thorough discussion on the magnetic properties of this family in the previous study.¹⁹ It is believed that the $d_\delta\text{--}p_\pi$ π conjugation within the six-membered $\text{Mo}_2/\text{chalcogen}$ core is the physical origin of the unusual magnetic behaviors.

Overall, the ^1H NMR spectra of **1** and **2** are similar to those of the protonated and deprotonated oxygen and sulfur derivatives, respectively. Let us focus on the downfield area of the spectra (Figures 4 and S1 and S2 in the Supporting

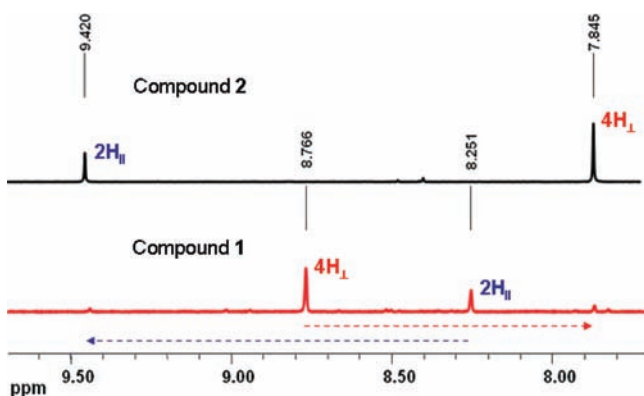


Figure 4. ^1H NMR spectra in CDCl_3 showing the downfield and upfield shifts for the in-plane (H_{\parallel}) and out-of-plane (H_{\perp}) methine protons (ArNCHNAr), respectively, upon oxidation and concomitant deprotonation of **1** (red) to **2** (black).

Information), where the two groups of methine protons, H_{\parallel} and H_{\perp} , show two singlets in a 1:2 ratio. For compound **1**, the H_{\parallel} 's resonate at a relatively high chemical shift in comparison with the H_{\perp} 's. The deviation of about 0.5 ppm in the chemical shift reflects the subtle difference in the microscopic, electronic, and magnetic environments for the H_{\parallel} and H_{\perp} protons. As shown in Figure 4, upon molecular transformation, the two signals at 8.766 ppm (H_{\perp}) and 8.251 ppm (H_{\parallel}) shifted toward opposite directions, arriving at 7.84 ppm (H_{\perp}) and 9.42 ppm (H_{\parallel}), respectively. Thus, in the spectrum of **2**, the NMR chemical shifts for the methine protons are considerably out of the normal range for paddlewheel dimolybdenum formamidate, for example, 8.38 ppm for the parent molecule $\text{Mo}_2(\text{DAniF})_4$.³⁴ The abnormality of the NMR chemical shifts for the protons in the vicinity of the $[\text{Mo}_2\text{E}_2\text{Mo}_2]$ core can be further manifested by comparison with the oxamidate-bridged dication, $\{\beta\text{-}[\text{Mo}_2(\text{DAniF})_3]_2(\text{oxamidate})\}^{2+}$. It has a central unit constructed by two fused six-membered Mo_2 chelating rings, which is furnished with 10 π electrons.³⁵ Similar to the system under investigation, this complex has two formal Mo_2^{5+} units but is diamagnetic because of the strong electronic interaction between the two dimetal units. However, the two sets of methine protons display a broad NMR signal at 8.6 ppm at -50°C .

For all three pairs with different bridging atoms, the downfield shift for the in-plane methine protons $[\Delta\delta(\text{H}_{\parallel})]$ is larger than the upfield shift for the out-of-plane methine protons $[\Delta\delta(\text{H}_{\perp})]$ (Table 3). It is noticeable that the NMR singlets for

Table 3. ^1H NMR (δ , ppm) Data for the Protons in Proximity to the Core and the Shielding Increments ($\Delta\delta$) Caused by the Core Conversion^a

^1H NMR (ppm)	$[\text{Mo}_2(\text{DAniF})_3]_2(\mu\text{-EH})_2$			$[\text{Mo}_2(\text{DAniF})_3]_2(\mu\text{-E})_2$		
	$\mu\text{-OH}$	$\mu\text{-SH}$	$\mu\text{-SeH}$	$\mu\text{-O}$	$\mu\text{-S}$	$\mu\text{-Se}$
$\delta(\text{H}_{\parallel})$	8.20	8.26	8.25	9.30	9.35	9.42
$\delta(\text{H}_{\perp})$	8.90	8.78	8.77	8.00	7.86	7.84
$\Delta\delta(\text{H}_{\parallel})$				1.10	1.09	1.17
$\Delta\delta(\text{H}_{\perp})$				-0.90	-0.92	-0.93
$\delta(\text{H}_{\parallel}) - \delta(\text{H}_{\perp})$	-0.7	-0.52	-0.52	1.30	1.49	1.58
$\delta(\text{H}_E)$	2.42	0.23	-2.39			

^a $\Delta\delta = \delta(2) - \delta(1)$.

H_{\parallel} and H_{\perp} protons in **2** are separated by about 1.58 ppm, larger than 1.49 and 1.30 ppm for the sulfur and oxygen analogues, respectively.¹⁹ This indicates that the selenium-bridged Mo_2 core has a larger impact on the neighboring protons, although the $\text{Mo}_2\cdots\text{Mo}_2$ separation is enlarged by the selenium atoms. It is also important to note that for the three precursors, which have a $[\text{Mo}_2(\text{EH})_2\text{Mo}_2]$ core ($\text{E} = \text{O}, \text{S}, \text{and Se}$), variation of the bridging atom E has a negligible influence on the chemical shifts for these protons (Table 3). Therefore, it is clear that abnormal NMR chemical shifts for the oxidized species should be attributed to the electron-delocalized six-membered $\text{Mo}_2/\text{chalcogen}$ ring.

Evaluation of Aromaticity for the $\text{Mo}_2/\text{Chalcogen Cores}$. With the addition of the selenium-bridged analogues, a family having three pairs of $\text{Mo}_2/\text{chalcogen}$ clusters has been developed, of which each pair consists of two molecules that can be assigned as nonaromatic and aromatic. The importance of the study on this system is the recognition that aromaticity may be realized through $d_{\delta}\text{-}p_{\pi}$ π conjugation without violation of the established principles in the field of aromaticity.

Interestingly, the processes of oxidation and deprotonation do not actually change the number of valence-shell electrons on the six-membered Mo_2/E core ($\text{E} = \text{O}, \text{S}, \text{and Se}$). For the two molecules in each pair, there are 30 valence electrons in total for the six ring-forming atoms. Scheme 4 interprets, in a

Scheme 4. Distributions of the Out-of-Shell Electrons on the Six-Membered Mo_2/E Core ($\text{E} = \text{O}, \text{S}, \text{and Se}$) for **1** and **2**

	$[\text{Mo}_2(\text{EH})_2\text{Mo}_2]$	$[\text{Mo}_2\text{E}_2\text{Mo}_2]$
d_{δ}	$2 \times 2 = 4$	$2 \times 1 = 2$
p_{π}	0	$2 \times 2 = 4$
E-H	$2 \times 1 = 2$	0
LP	$2 \times 2 = 4$	$2 \times 2 = 4$
π	$2 \times 2 \times 2 = 8$	$2 \times 2 \times 2 = 8$
σ	$6 \times 2 = 12$	$6 \times 2 = 12$

localized model, the distribution of these electrons on the two distinct six-membered central units. The deprotonated $[\text{Mo}_2\text{E}_2\text{Mo}_2]$ core has six π electrons, two from the Mo_2 units (δ) and four from the bridging E (p_{π}), and a sp^2 lone pair on each of the E atoms. For the precursors, the core has two δ electrons on each $[\text{Mo}_2]$ unit, one σ -bonding electron (E-H) and one pseudo- sp^3 lone pair on each of the two bridging E atoms. Through satisfaction of Hückel's $(4n + 2)$ rule, the deprotonated molecules exhibit aromatic character, which is in contrast to the protonated precursors.

Therefore, the two molecules in each pair become valence isomers that are barely seen, especially in inorganic compounds. They somehow resemble a well-known pair of molecules, Dewar benzene and benzene. Structurally, in Dewar benzene, a

pair of C=C double bonds is bridged by two carbon atoms through σ bonds. Similarly, in this Mo_2/E family, the nonaromatic species has two $\text{Mo}\equiv\text{Mo}$ quadruple bonds linked by two chalcogen atoms (O, S, or Se) via σ -type coordination bonds. Oxidation/deprotonation triggered the structural alternation of the core. Similarly, sp^3 hybridization of the two carbon atoms in Dewar benzene is changed to sp^2 as it is converted into benzene. As is known, for benzene, there is no alternative arrangement of single and double C–C bonds because of cyclic π conjugation. Theoretical work has proven that the Mo–E bonds (E = O and S) are no longer coordination single bonds and the bond order is almost doubled. On the other hand, this Mo_2 system has a three-dimensional molecular skeleton with multiple chelating rings fused through two Mo–Mo multiple bonds. It is interesting that, for such a sophisticated dimetal complex system, the central fragment of the molecule, e.g., the $[\text{Mo}_2\text{E}_2\text{Mo}_2]$ core, governs electronically and magnetically over the entire molecule, displaying major characters similar to that of benzene.

In view of bonding interaction, the aromaticity of this Mo_2 system should be attributed to the similarity between the π component in a C–C double bond and the δ component in a Mo_2 quadruple bond. They are both $2c-2e$ bonds associated with the HOMO in the corresponding unsaturated bond category. More importantly, the δ and π bonds, including their bonding and antibonding orbitals, share the common symmetry property that is necessary for π -orbital interactions. In the $[\text{Mo}_2\text{E}_2\text{Mo}_2]$ unit, cyclic π conjugation is pervaded through $d_\delta-p_\pi$ interaction, as in benzene by the $p_\pi-p_\pi$ interaction. This speculation is confirmed by the similarity of the frontier MOs for the complexes and benzene.

While the $[\text{Mo}_2\text{E}_2\text{Mo}_2]$ cores with different chalcogen atoms serving as the bridges generally exhibit aromatic character, it appears that there is a gradual increase in the degree of aromaticity for the three analogues having bridging atoms in order from oxygen to selenium. The selenium-bridged molecule shows the largest ^1H NMR deviations for the two sets of *methine* protons and the lowest energy for the metal-to-ligand (E) charge transfer. These data consistently suggest that selenium bridging leads to a higher degree of electronic delocalization, thus inducing a magnetic anisotropy larger than that from any other $\text{Mo}_2/\text{chalcogen}$ core. While aromaticity is considered to be a vexing property because it is hardly gauged quantitatively, it is generally accepted that diamagnetic anisotropy, as measured by the difference between the diatropic and paratropic components of diamagnetic susceptibility ($\Delta\chi$), is a semiquantitative criterion that correlates the degree of aromaticity with the NMR chemical shift of the protons in proximity to the aromatic entity.³⁶ The correlation of the magnetic shielding effect (shielding tensor σ) with the diamagnetic anisotropy arising from cyclic π conjugation was established by the McConnell equation in an earlier work,³⁷ which was used to estimate shielding from the benzene ring. If the increment of the shielding tensor ($\Delta\sigma$) is replaced by the chemical shift change ($\Delta\delta$), or $\Delta\delta = -\Delta\sigma$, the McConnell equation can be expressed as follows:

$$\Delta\delta = \Delta\chi[(3 \cos 2\theta - 1)/3R^3N]$$

where R is the distance (\AA) from the center of the aromatic plane to the proton interested, θ is the angle between vector R and the symmetry axis perpendicular to the ring, N is

Avogadro's number, and $\Delta\chi$ is the anisotropy of molecular magnetic susceptibility (ppm cgs) defined by

$$\Delta\chi = \chi_{zz} - \frac{1}{2}(\chi_{xx} + \chi_{yy}) = \chi_{\perp} - \chi_{\parallel}$$

where χ_{zz} , χ_{xx} , and χ_{yy} are the magnetic susceptibility components corresponding to the z , x , and y axes in Cartesian coordinates, respectively. By taking the z axis normal to the molecular plane, the out-of-plane component χ_{\perp} equals χ_{zz} and the in-plane component χ_{\parallel} is representative of χ_{xx} and χ_{yy} .

For the aromatic species (**2**), the distance of the in-plane *methine* protons (H_{\parallel}) from the centroid of the $[\text{Mo}_2\text{Se}_2\text{Mo}_2]$ ring (R) is 6.04 \AA and the R vector is perpendicular to the main axis C_2 ($\theta = 90^\circ$; Figure 5). The change of the chemical shift

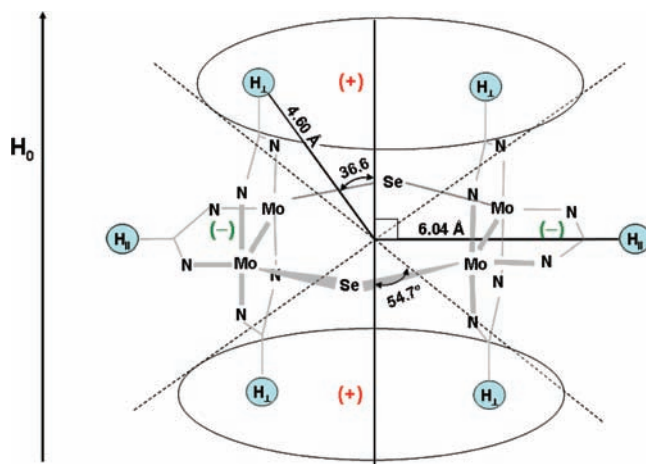


Figure 5. Diamagnetic anisotropy induced by the $[\text{Mo}_2\text{Se}_2\text{Mo}_2]$ ring in **2** as an example for complexes $[\text{Mo}_2(\text{DAniF})_3]_2(\mu\text{-E})_2$ (E = O, S, and Se). For *methine* hydrogen atoms from the ancillary DAniF ligands, those labeled H_{\parallel} are essentially coplanar with the six-membered $\text{Mo}_2/\text{chalcogen}$ ring, while those labeled H_{\perp} are perpendicular to this plane. According to McConnell, the sign of the anisotropic magnetic field changes at $\theta = 54.7^\circ$. Thus, H_{\parallel} ($\theta = 90^\circ$) and H_{\perp} ($\theta = 36.6^\circ$) are located in the deshielding (–) and shielding (+) zones, respectively, which is consistent with the ^1H NMR spectra.

($\Delta\delta$) may be measured by referring to that of the nonaromatic counterpart **1**. However, the Mo–Mo multiple bonds generate local magnetic perturbations that significantly influence the chemical shifts for the concerned protons. This local anisotropic magnetic field has the negative cone in the equatorial area and the positive cone in the axial direction with respect to the metal–metal multiple bond.^{24,34,38} This is why the *methine* protons on $\text{Mo}_2(\text{DAniF})_4$ resonate at 8.38 ppm, while for the dimetal compounds without metal–metal bonding interaction, the ^1H NMR signals appear in a relatively high field, for example, 6.16 ppm for $\text{Ni}_2(\text{form})_4$ and 7.05 ppm for $\text{Pd}_2(\text{form})_4$ [form = *N,N'*-bis(*p*-methylphenyl)-fomamidinate].³⁹ Therefore, for the $[\text{Mo}_2]$ building blocks, the protons on the ancillary ligands generally experience significant deshielding. For the same reason, we have seen that, for this system, the shielding increment for the in-plane *methine* protons is larger than that for the out-of-plane ones (Table 4). In order to take into account this local deshielding effect, we chose to use 8.38 ppm for the *methine* protons in $\text{Mo}_2(\text{DAniF})_4$ as the “zero point” to measure the NMR deviations for the calculations. Thereby, a downfield shift of 1.04 ppm for the in-plane *methine* protons, or $\Delta\delta(\text{H}_{\parallel}) = 9.42-8.38$ ppm, is

Table 4. $\Delta\chi$ Values Calculated from the McConnell Equation for the Three Aromatic Species^a

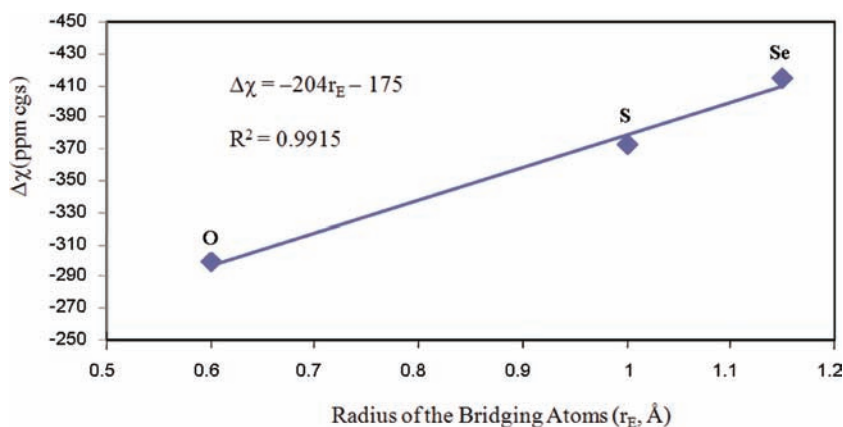
	$\Delta\delta$ (ppm) ^b	R (Å)	θ (deg)	$\Delta\chi$ (ppm cgs)
$[\text{Mo}_2(\text{DAniF})_3]_2(\mu\text{-O})_2$	-0.93	5.623	90	-299
$[\text{Mo}_2(\text{DAniF})_3]_2(\mu\text{-S})_2$	-0.97	5.970	90	-373
$[\text{Mo}_2(\text{DAniF})_3]_2(\mu\text{-Se})_2$	-1.04	6.036	90	-414

^aFor each case, the calculations were based on the experimental data associated with the in-plane *methine* protons (H_{\parallel}). ^b $\Delta\delta$ was calculated by referencing to the chemical shift of the *methine* protons of $\text{Mo}_2(\text{DAniF})_4$ (8.38 ppm).

obtained. Because the aromatic species and its reference molecule share a common molecular topology and have similar structural parameters, we assume that the other local magnetic effects are essentially canceled and the downfield shift is dominantly due to the contribution of the six mobile π electrons within the $[\text{Mo}_2\text{Se}_2\text{Mo}_2]$ core. Thus, according to the McConnell equation, the change of the diamagnetic susceptibility $\Delta\chi$ is calculated to be -414 ppm cgs. One might be surprised with this result because it means that the magnetic anisotropy induced by the $[\text{Mo}_2\text{Se}_2\text{Mo}_2]$ core is about 6-fold as large as that for benzene (-62.9 ppm cgs). However, this abnormally large diamagnetic anisotropy explains well the unusually long-range shielding effect. The shielding of the benzene is generally estimated from the NMR chemical shift (δ) of the protons, which is about 2 ppm downfield relative to the signals for ethylene protons. However, it should be noted that the benzene proton is much closer to the ring center (ca. 2.45 Å). To evaluate the long-range deshielding effect of benzene, we may calculate the chemical shift (δ) for six imaginary coplanar protons at a distance of 6.04 Å under the same magnetic anisotropic field, e.g., $\Delta\chi = -62.9$ ppm cgs. Calculation from the McConnell equation gives a downfield shift ($\Delta\delta$) of 0.023 ppm, meaning that the long-range deshielding from the benzene ring is very weak. The NMR chemical shift for these "protons" would be 5.30 ppm (5.28 + 0.023) rather than 7.28 ppm of the benzene protons. As a matter of fact, in the present case, all of the protons on the DAniF ligands, including those from the methoxyl groups (OCH_3), which are separated from the center of the ring by about 10 Å, are affected by the induced anisotropic magnetic field. Their NMR chemical shifts are displaced accordingly with respect to the corresponding signals for the precursor (see Figures S1 and S2 in the Supporting Information). As is known,

the $\Delta\chi$ values for two fused double-ring molecules, naphthalene and azulene, are 130.3 and 144.0 ppm cgs, respectively.²⁵ Therefore, the results from the McConnell equation suggest that the deshielding for the in-plane protons in proximity to the $[\text{Mo}_2\text{Se}_2\text{Mo}_2]$ ring is dramatically larger than that for the benzenoid system.

According to the McConnell equation, the sign of the magnetic field induced by the Mo₂/Se core changes at $\theta = 54.7^\circ$. In **2**, the four *methine* protons on the perpendicular DAniF are situated above and below the $[\text{Mo}_2\text{Se}_2\text{Mo}_2]$ plane at angle $\theta = 36.6^\circ$ (Figure 5). Therefore, it is expected that these protons experience a shielding instead. This is consistent with the experimental observation that the NMR for the H_{\perp} 's moved from 8.766 to 7.845 ppm. Given the magnitude of the magnetic anisotropy $\Delta\chi$ (-414 ppm cgs) and the distance (R) 4.6 Å, as measured from the crystal structure, calculation from the McConnell equation predicts a change of the chemical shift for these protons, $\Delta\delta_{\text{cal}}(H_{\perp}) = -2.20$ ppm. At first glance, this might be another surprising result compared to the experimental observation, that is, $\Delta\delta_{\text{exp}}(H_{\perp}) = -0.93$ ppm. It should be noted that, in the calculation, the local magnetic perturbations from the Mo-Mo multiple bond were not considered and the resulting $\Delta\delta_{\text{cal}}(H_{\perp})$ does not include the deshielding sensed by these protons. In order to estimate the net NMR upfield shift for the H_{\perp} 's, the opposite effect should be added. Electronically, the nonbonding dipalladium $\text{Pd}_2(\text{form})_4$ is preferable as the reference compound to evaluate the deshielding effect caused by the Mo-Mo quadruple bonds. With 7.05 ppm for the *methine* protons in $\text{Pd}_2(\text{form})_4$ and 8.38 ppm for those in $\text{Mo}_2(\text{DAniF})_4$, the Mo₂ deshielding effect is estimated to be 1.23 ppm. For an approximate treatment, offsetting 1.23 ppm from $\Delta\delta_{\text{cal}}(H_{\perp})$ (-2.20 ppm) yields a net δ change of -0.97 ppm for the four H_{\perp} 's. It is remarkable that the observed NMR displacement from 8.776 to 7.845 ppm for the H_{\perp} 's, or a δ deviation of -0.93 ppm, is in excellent agreement with the calculated result from the McConnell equation. On this basis, the estimated abnormally large diamagnetic anisotropy $\Delta\chi = -414$ ppm cgs for the six-membered aromatic $[\text{Mo}_2\text{Se}_2\text{Mo}_2]$ unit is considered to be acceptable. On the other hand, the evaluation of $\Delta\chi$ is made here based on a through-space-only model and substantial assumptions. Some factors that can possibly affect the shielding tensor of the magnetic anisotropy, for example, the heteronuclearity of the ring system, the local influences from

**Figure 6.** Plot of the calculated $\Delta\chi$ values from the McConnell equation versus the atomic radius of the bridging atoms E in $[\text{Mo}_2(\text{DAniF})_3]_2(\mu\text{-E})_2$ (E = O, S, and Se).

the Mo-DAniF chelating rings, and so on, have not been fully taken into account. Nevertheless, this preliminary analysis shows that cyclic π delocalization over the $[\text{Mo}_2\text{E}_2\text{Mo}_2]$ core makes the dominant contributions to the proton chemical shifts and the ring-current model accounts well for the long-range magnetic anisotropy.

By employment of the McConnell equation, calculations of $\Delta\chi$ for the three aromatic molecules from each pair were performed (Table 4). Interestingly, it is found that the magnitude of $\Delta\chi$ for the $\text{Mo}_2/\text{chalcogen}$ core is a function of the atomic radius of the bridging elements (r_E). Figure 6 is a plot of $\Delta\chi$ versus r_E . The linear relationship between $\Delta\chi$ and r_E is supported by the satisfactorily related coefficient 0.992. This result is in agreement with the experimental observations that the $[\text{Mo}_2\text{Se}_2\text{Mo}_2]$ core has the largest anisotropic impact on the surrounding protons. This aromaticity sequence is consistent with that observed for the chalcogen-containing five-membered ring system, in which the aromaticity is ordered as furan < thiophene < selenophene. As measured by diamagnetic susceptibility exaltation, furan is considerably less aromatic than benzene, but the aromaticity for selenophene is greater than that for benzene.⁴⁰ The trend of $\Delta\chi$ varying with the atomic radius is understandable because the π -orbital interactions are optimized as the heavier atom is introduced, consequently enhancing the aromaticity. In comparison with benzene, the $\text{Mo}_2/\text{chalcogen}$ core is constructed by six heavier ring-forming atoms including two sets of Mo_2 units; thus, cyclic π conjugation engenders a higher degree of aromaticity.

CONCLUSION

In the present work, the δ aromaticity associated with Mo–Mo multiple bonds is further discussed based on the preparation and characterization of two selenium-bridged valence isomers, **1** and **2**. While the molecular topology is retained, aerobic oxidation of the quadruple Mo–Mo bonds triggered the Mo_2/Se core conversion from $[\text{Mo}_2(\text{SeH})_2\text{Mo}_2]$ to $[\text{Mo}_2\text{Se}_2\text{Mo}_2]$. It is confirmed, according to conventional aromatic criteria, that the molecule having a six-membered $[\text{Mo}_2\text{Se}_2\text{Mo}_2]$ central unit is aromatic, distinct from its precursor, which has a $[\text{Mo}_2(\text{SeH})_2\text{Mo}_2]$ core. The selenium-bridged core has a greater impact on the protons in its vicinity than the other two $\text{Mo}_2/\text{chalcogen}$ cores. From the McConnell equation, the induced diamagnetic anisotropy ($\Delta\chi$) for the $[\text{Mo}_2\text{Se}_2\text{Mo}_2]$ core is estimated to be -414 ppm cgs, which is dramatically larger than that for benzene. The large magnitude of $\Delta\chi$ conforms well with the abnormal NMR chemical shifts for the protons in proximity to the core, although this may not be the only possible explanation. We attribute the aromatic character of the $\text{Mo}_2/\text{chalcogen}$ core to the analogy in the bonding nature between the δ orbital in the metal–metal quadruple bond and the π orbital in the C–C double bond. On this basis, the physical origin of aromaticity is exemplified and the conventional ring-current model is validated through this non-carbon complex system.

EXPERIMENTAL SECTION

Materials and Methods. Solvents used were freshly distilled under N_2 by employing standard procedures or dried and degassed using a Vacuum Atmospheres Company solvent purification system. All synthetic operations were conducted under N_2 using Schlenk-line techniques. The starting material $\text{Mo}_2(\text{DAniF})_3(\text{O}_2\text{CCH}_3)$ was prepared by following a published method.²⁶ Commercially available chemicals were used as received.

Physical Measurements. Elemental analyses were performed by The Analytical Center at Sun Yat-Sen University, Guangzhou, China. Electronic spectra of **1** and **2** in dichloromethane were measured in the range of 300–1000 nm on a Shimadzu UV-2501PC spectrophotometer. ^1H NMR spectra were recorded on a Bruker-400 NMR spectrometer with chemical shifts (δ , ppm) referenced to CDCl_3 . Cyclic voltammograms were obtained by measurement of **2** in a dichloromethane solution on a CH Instruments electrochemical analyzer with platinum working and auxiliary electrodes and an Ag/AgCl reference electrode, using a scan rate of 100 mV s^{-1} and $0.1 \text{ M Bu}_4\text{NPF}_6$ as an electrolyte.

Preparation of $[\text{Mo}_2(\text{DAniF})_3]_2(\mu\text{-SeH})_2$ (1**).** A total of 0.160 g (2.0 mmol) of the element selenium was reacted with 0.068 g of NaBH_4 (2.0 mmol) in 15 mL of ethanol for 1 h until the solids disappeared.⁴¹ While stirring, the obtained NaHSe solution was transferred through a cannula to a Schlenk flask having 0.408 g (0.40 mmol) of $\text{Mo}_2(\text{DAniF})_3(\text{O}_2\text{CCH}_3)$ in 40 mL of THF. The mixture was then stirred at ambient temperature for 4 h, generating a brownish solution. After removal of the solvent under reduced pressure, the residue was washed with ethanol ($3 \times 15 \text{ mL}$) and then dried under vacuum. The crude solid product was dissolved in dichloromethane (10 mL), and the solution was layered with ethanol. Brownish-yellow crystals formed after 4 days. Yield: 0.235 g (56.6%). ^1H NMR (CDCl_3 , ppm): δ 8.46 (s, 4H, NCHN), 8.38 (s, 2H, NCHN), 6.64 (m, 16H, aromatic), 6.51 (m, 16H, aromatic), 6.42 (d, 8H, aromatic), 6.20 (d, 8H, aromatic), 3.72 (s, 24H, OCH_3), 3.66 (s, 12H, OCH_3). UV–vis [CH_2Cl_2 ; λ_{max} , nm (ϵ , $\text{M}^{-1} \text{cm}^{-1}$): 451 (5.95×10^3). Anal. Calcd for $\text{C}_{90}\text{H}_{92}\text{N}_{12}\text{O}_{12}\text{Se}_2\text{Mo}_4$ (**1**): C, 52.08; H, 4.47; N, 8.10. Found: C, 52.02; H, 4.51; N, 8.16.

Preparation of $[\text{Mo}_2(\text{DAniF})_3]_2(\mu\text{-Se})_2$ (2**).** To a yellow solution prepared by dissolving 0.240 g of **1** (0.10 mmol) in 10 mL of CH_2Cl_2 was injected 20 mL of air using a syringe. This mixture was stirred at room temperature for 4 h, during which the color of the solution changed from yellow to dark brown. The addition of sufficient hexanes to the solution produced brown precipitates, followed by a routine treatment. The crude product was obtained essentially quantitatively. Dark single crystals of $2 \cdot 2\text{CH}_2\text{Cl}_2$ were obtained by diffusion of hexanes into the dichloromethane solution. Yield: 0.11 g (56%). ^1H NMR (CDCl_3 , ppm): δ 9.42 (s, 2H, NCHN), 7.84 (s, 4H, NCHN), 6.45–6.48 (m, 24H, aromatic), 6.36 (m, 16H, aromatic), 6.22 (d, 8H, aromatic), 3.68 (s, 12H, OCH_3), 3.62 (s, 24H, OCH_3). UV–vis [CH_2Cl_2 ; λ_{max} , nm (ϵ , $\text{M}^{-1} \text{cm}^{-1}$): 451 (5.95×10^3). Anal. Calcd for $\text{C}_{90}\text{H}_{90}\text{N}_{12}\text{O}_{12}\text{Se}_2\text{Mo}_4$ (**2**): C, 52.13; H, 4.38; N, 8.11. Found: C, 52.28; H, 4.44; N, 8.42.

X-ray Structure Determinations. For each compound, a single crystal suitable for X-ray diffraction analysis was sealed in a quartz fiber and attached to the goniometer head. Data for $1 \cdot 2\text{CH}_2\text{Cl}_2$ and $2 \cdot 2\text{CH}_2\text{Cl}_2$ were collected at 293 K on a Bruker SMART 1000 CCD area detector system. Cell parameters were determined using the program SMART.⁴² Data reduction and integration were performed with software package SAINT,⁴³ which corrects for Lorentz and polarization effects, while absorption corrections were applied using the program SADABS.⁴⁴ The positions of the non-hydrogen atoms were found using the direct methods program in the Bruker SHELXTL software package. Subsequent cycles of least-squares refinement, followed by difference Fourier syntheses, revealed the positions of the remaining non-hydrogen atoms. Hydrogen atoms, except for those on the hydroselenyl groups (SeH) of **1**, were added in idealized positions. Non-hydrogen atoms were refined with anisotropic displacement parameters. Some of the anisyl groups in the DAniF ligands and interstitial CH_2Cl_2 molecules were found disordered in $1 \cdot 2\text{CH}_2\text{Cl}_2$ and $2 \cdot 2\text{CH}_2\text{Cl}_2$, and they were refined with soft constraints. Crystal data and structural refinement information are given in Table 1. Selected distances and angles are given in Table 2. Other crystallographic data are given in the Supporting Information.

■ ASSOCIATED CONTENT

■ Supporting Information

Crystallographic data in CIF format and ^1H NMR spectra. This material is available free of charge via the Internet at <http://pubs.acs.org>.

■ AUTHOR INFORMATION

Corresponding Author

*E-mail: cyluu06@mail.tongji.edu.cn. Fax: (011)86-21-65985153.

■ ACKNOWLEDGMENTS

We thank the National Science Foundation of China (Grants 20871093 and 90922010), Tongji University, Jinan University, and Sun Yat-Sen University for financial support.

■ REFERENCES

- (1) (a) Krygowski, T. M.; Cyrański, M. K. *Chem. Rev.* **2001**, *101*, 1385. (b) Heine, T.; Corminboeuf, C.; Seifert, G. *Chem. Rev.* **2005**, *105*, 3889. (c) Gomes, J. A. N. F.; Mallion, R. B. *Chem. Rev.* **2001**, *101*, 1349. (d) Katritzky, A. R.; Jug, K.; Oniciu, D. C. *Chem. Rev.* **2001**, *101*, 1421.
- (2) (a) Kekulé, A. *Bull. Soc. Chim. Paris* **1865**, *3*, 98. (b) Kekulé, A. *Ann.* **1866**, *137*, 129. (c) Kekulé, A. *Ann.* **1872**, *162*, 77.
- (3) (a) Hückel, E. Z. *Physik* **1931**, *70*, 204 and 72–310. (b) Pauling, L. J. *Chem. Phys.* **1936**, *4*, 673. (c) London, F. J. *Phys. Radium* **1933**, *8*, 397. (d) Pople, J. A. J. *Chem. Phys.* **1956**, *24*, 1111. (e) Armit, J. W.; Robinson, R. J. *Chem. Soc.* **1925**, *127*, 1604.
- (4) Balaban, A. T.; Oniciu, D. C.; Katritzky, A. R. *Chem. Rev.* **2004**, *104*, 2777.
- (5) Thorn, D. L.; Hoffmann, R. *Nouv. J. Chim.* **1979**, *3*, 39.
- (6) Elliott, G. P.; Roper, W. R.; Waters, J. M. J. *Chem. Soc., Chem. Commun.* **1982**, 811.
- (7) Xia, H.; He, G.; Zhang, H.; Wen, T. B.; Sung, H. H. Y.; Williams, I. D.; Jia, G. J. *Am. Chem. Soc.* **2004**, *126*, 6862.
- (8) (a) Bleeke, J. R.; Xie, Y. F.; Peng, W. J.; Chiang, M. J. *Am. Chem. Soc.* **1989**, *111*, 4118. (b) Bleeke, J. R. *Acc. Chem. Res.* **2007**, *40*, 1035. (c) Bleeke, J. R.; Behm, R.; Xie, Y.; Chiang, M. Y.; Robinson, K. D.; Beatty, A. M. *Organometallics* **1997**, *16*, 606.
- (9) (a) Landorf, C. W.; Jacob, V.; Weakley, T. J. R.; Haley, M. M. *Organometallics* **2004**, *23*, 1174. (b) Bleeke, J. R. *Acc. Chem. Res.* **1991**, *24*, 271.
- (10) (a) Ashe, A. J. III. *Acc. Chem. Res.* **1978**, *11*, 153. (b) Takeda, N.; Shinohara, A.; Tokitoh, N. *Organometallics* **2002**, *21*, 4024. (c) Mizuhata, Y.; Noda, N.; Tokitoh, N. *Organometallics* **2010**, *29*, 4781.
- (11) Bleeke, J. R. *Chem. Rev.* **2001**, *101*, 1205.
- (12) Steiner, E.; Fowler, P. W. J. *Phys. Chem. A* **2001**, *105*, 9553.
- (13) Fernández, I.; Frenking, G. *Chem.—Eur. J.* **2007**, *13*, 5873.
- (14) Periyasamy, G.; Burton, N. A.; Hillier, I. H.; Thomas, J. M. H. J. *Phys. Chem. A* **2008**, *112*, 5960.
- (15) (a) Schleyer, P. v. R.; Maerker, C.; Dransfeld, A.; Jiao, H. J.; Hommes, N. J. R. v. E. J. *Am. Chem. Soc.* **1996**, *118*, 6317. (b) Chen, Z. F.; Wannere, C. S.; Corminboeuf, C.; Puchta, R.; Schleyer, P. v. R. *Chem. Rev.* **2005**, *105*, 3842.
- (16) Landorf, C. W.; Haley, M. M. *Angew. Chem., Int. Ed.* **2006**, *45*, 3914.
- (17) Cotton, F. A.; Murillo, C. A.; Walton, R. A. *Multiple Bonds between Metal Atoms*; Springer Science and Business Media, Inc.: New York, 2005.
- (18) Cotton, F. A.; Nocera, D. G. *Acc. Chem. Res.* **2000**, *33*, 483.
- (19) Fang, W.; He, Q.; Tan, Z. F.; Liu, C. Y.; Lu, X.; Murillo, C. A. *Chem.—Eur. J.* **2011**, *17*, 10288.
- (20) (a) Tamelen, E. E. v. *Acc. Chem. Res.* **1971**, *5*, 186. (b) Tamelen, E. E. v.; Pappas, S. P.; Kirk, K. L. J. *Am. Chem. Soc.* **1971**, *93*, 6092.
- (21) Viglione, R. G.; Zanasi, R. *Org. Lett.* **2004**, *6*, 2265.
- (22) Wannere, C. S.; Schleyer, P. v. R. *Org. Lett.* **2003**, *5*, 605.

(23) Harris, R. K. *Nuclear Magnetic Resonance Spectroscopy*; Pittman: London, 1983.

(24) (a) Cotton, F. A.; Ren, T. J. *Am. Chem. Soc.* **1992**, *114*, 2237. (b) Cotton, F. A.; Daniels, L. M.; Lei, P.; Murillo, C. A.; Wang, X. *Inorg. Chem.* **2001**, *40*, 2778.

(25) Schleyer, P. v. R.; Jiao, H. *Pure Appl. Chem.* **1996**, *68*, 209.

(26) Cotton, F. A.; Liu, C. Y.; Murillo, C. A.; Villagrán, D.; Wang, X. *J. Am. Chem. Soc.* **2003**, *125*, 13564.

(27) (a) Cotton, F. A.; Dalal, N. S.; Liu, C. Y.; Murillo, C. A.; North, J. M.; Wang, X. *J. Am. Chem. Soc.* **2003**, *125*, 12945. (b) Cotton, F. A.; Li, Z.; Liu, C. Y.; Murillo, C. A.; Villagrán, D. *Inorg. Chem.* **2006**, *45*, 767.

(28) Cotton, F. A.; Li, Z.; Murillo, C. A.; Wang, X.; Yu, R.; Zhao, Q. *Inorg. Chem.* **2007**, *46*, 3245.

(29) Cotton, F. A.; Li, Z.; Liu, C. Y.; Murillo, C. A.; Villagrán, D. *Inorg. Chem.* **2006**, *45*, 767.

(30) (a) Ren, T. *Organometallics* **2005**, *24*, 4854. (b) Chisholm, M. H.; Patmore, N. J. *Acc. Chem. Res.* **2007**, *40*, 19. (c) Cotton, F. A.; Li, Z.; Liu, C. Y.; Murillo, C. A.; Villagrán, D. *Inorg. Chem.* **2006**, *45*, 767. (d) Cotton, F. A.; Murillo, C. A.; Villagrán, D.; Yu, R. J. *Am. Chem. Soc.* **2006**, *128*, 3281. (e) Han, M. J.; Liu, C. Y.; Tian, P. F. *Inorg. Chem.* **2009**, *48*, 6347.

(31) (a) Chisholm, M. H.; Macintosh, A. M. *Chem. Rev.* **2005**, *105*, 2949. (b) Cotton, F. A.; Lin, C.; Murillo, C. A. *Acc. Chem. Res.* **2001**, *34*, 759. (c) Cotton, F. A.; Lin, C.; Murillo, C. A. *Proc. Natl. Acad. Sci. U.S.A.* **2002**, *99*, 4810.

(32) Cotton, F. A.; Li, Z.; Liu, C. Y.; Murillo, C. A.; Zhao, Q. *Inorg. Chem.* **2006**, *45*, 6387.

(33) Mitchell, R. H. *Chem. Rev.* **2001**, *101*, 1301.

(34) Lin, C.; Protasiewicz, J. D.; Smith, E. T.; Ren, T. *Inorg. Chem.* **1996**, *35*, 6422.

(35) Cotton, F. A.; Liu, C. Y.; Murillo, C. A.; Villagrán, D.; Wang, X. *J. Am. Chem. Soc.* **2004**, *126*, 14822.

(36) (a) Benson, R. C.; Norris, C. L.; Flygare, W. H.; Beak, P. J. *Am. Chem. Soc.* **1971**, *93*, 5591. (b) Fleischer, U.; Kutzelnigg, W.; Lazzeretti, P.; Mühlenkamp, V. J. *Am. Chem. Soc.* **1994**, *116*, 5298.

(37) McConnell, H. M. J. *Chem. Phys.* **1957**, *27*, 226.

(38) San Filippo, J. *Inorg. Chem.* **1972**, *11*, 3140.

(39) Cotton, F. A.; Matusz, M.; Poli, R.; Feng, X. J. *Am. Chem. Soc.* **1988**, *110*, 1144.

(40) Pozharskii, A. F. *Chem. Heterocycl. Compd.* **1986**, *21*, 717.

(41) Klayman, D. L.; Griffin, T. S. J. *Am. Chem. Soc.* **1973**, *95*, 197.

(42) SMART, version 5.05; Bruker Analytical X-ray System, Inc.: Madison, WI, 1998.

(43) SAINT, *Data Reduction Software*, version 6.28A; Bruker Analytical X-ray Systems, Inc.: Madison, WI, 2001.

(44) SADABS, *Area Detector Absorption and Other Corrections*, version 2.03; Bruker Advanced X-ray Solutions, Inc.: Madison, WI, 2002.

■ NOTE ADDED AFTER ASAP PUBLICATION

This paper was published on the Web on February 1, 2012, with minor errors in equation 2. The corrected version was reposted on February 2, 2012.